Turbulent Fluctuations with the Electron Gyro-Scale in NSTX Plasmas

E. Mazzucato,[1,*] **R. E. Bell,**[1] **C. W. Domier,**[3] **S. Ethier,**[1] **J. C. Hosea,**[1] **S. M. Kaye,**[1] **B. P. LeBlanc,**[1] **W. Lee,**[5] **N. C. Luhmann, Jr.,**[3] **D, Mikkelsen,**[1] **H. Park,**[5] **P. M. Ryan,**[2] **D. R. Smith,**[1] **W. M. Tang,**[1] **G. Taylor,**[1] **W. Wang,**[1] **J. R. Wilson,**[1] **H. Yuh**[4] **and the NSTX Group**

[1]Princeton Plasma Physics Laboratory, Princeton University, Princeton, New Jersey 08543, USA
[2]Oak Ridge National Laboratory, Oak Ridge, Tennessee 37831, USA
[3]University of California at Davis, Davis, California 95616, USA
[4]Nova Photonics Inc., Princeton, NJ 08540, USA
[5]Department of Physics, POSTECH, Pohang 790-784, Korea

*E-mail: mazzucato@pppl.gov

Abstract

Various theories and numerical simulations support the conjecture that the ubiquitous problem of anomalous electron transport in tokamaks may arise from an electron gyro-scale turbulence driven by the electron temperature gradient. To check whether such turbulence is present in plasmas of the National Spherical Torus Experiment (NSTX), measurements of turbulent fluctuations were performed with coherent scattering of electromagnetic waves. Results from plasmas heated by high harmonic fast waves (HHFW) confirm the existence of density fluctuations in the range of wave numbers $k_\perp \rho_e = 0.1\text{-}0.4$, corresponding to a turbulence scale length of the order of the collisionless skin depth. Experimental observations and agreement with numerical results from a linear gyrokinetic stability code indicate that the observed turbulence is indeed driven by the electron temperature gradient.

1. Introduction

Understanding the mechanism of plasma transport in tokamaks is one of the great challenges of fusion research. Indeed, since most explanations of this phenomenon are based on some type of turbulence [1-3], understanding plasma transport is tantamount to understanding turbulence. Unfortunately, since this is a tremendously difficult problem, the cause of anomalous energy losses in tokamaks is still an outstanding issue.

Particularly difficult to explain is the transport of electron energy. This is the most worrisome since in a tokamak reactor a large fraction of the energy of charged fusion products – necessary to sustain the fusion reactions – would be released directly to the electrons. Various theories and numerical simulations [4–9] support the conjecture that anomalous electron transport may arise from an electron gyro-scale turbulence driven by the Electron Temperature Gradient (ETG) instability. However, even though a limited circumstantial evidence has been presented in [10] on the role of the ETG turbulence in

transport of plasma in Tore Supra, and measurements on FT-2 of fluctuations with an electron gyro-scale have been reported in [11], the existence of a turbulence driven by the electron temperature gradient has never been proved experimentally in tokamaks.

To investigate this type of turbulence, a series of experiments have been performed in plasmas of the National Spherical Torus Experiment (NSTX). These plasmas are uniquely suited for the study of the physics of electron transport since, while the confinement of ions in NSTX is very often at or near neoclassical levels, that of electrons is anomalous in all operational regimes [12]. Preliminary results from these experiments have been presented in [13]. Here we give a more detailed description of our measurements of short scale turbulent fluctuations driven by the electron temperature gradient in NSTX plasmas.

2. Coherent scattering of e.m. waves

Short scale plasma density fluctuations were measured with coherent scattering of electromagnetic waves, a process that can be charac-

terized by an effective differential cross section per unit volume

$$\sigma = r_0^2 S(\boldsymbol{k}, \omega), \qquad (1)$$

where $r_0 = e^2/mc^2$ is the classical radius of electrons and $S(\boldsymbol{k}, \omega)$ is the spectral density of fluctuations [14]. The mean square plasma density fluctuation is obtained from

$$\left\langle |\tilde{n}_e|^2 \right\rangle = \frac{1}{(2\pi)^4} \int S(\boldsymbol{k}, \omega) d\boldsymbol{k} d\omega, \qquad (2)$$

Frequency (ω) and wave vector ($\boldsymbol{k}$) of fluctuations must satisfy the energy and momentum conservation, i.e., $\omega = \omega_s - \omega_i$ and $\boldsymbol{k} = \boldsymbol{k}_s - \boldsymbol{k}_i$, where superscripts s and i refer to scattered and incident waves, respectively. Since for the topic of this paper $\omega_s \approx \omega_i$ and $k_s \approx k_i$, the scattering angle θ must satisfy the Bragg condition

$$k = 2k_i \sin(\theta/2). \qquad (3)$$
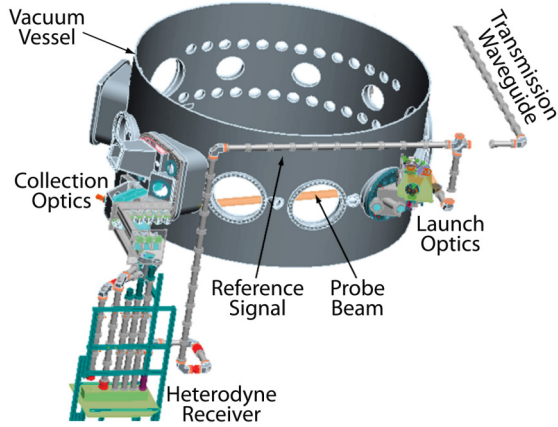
**Figure 1**. Schematic illustration of the scattering apparatus showing some of the major hardware components.

The NSTX scattering system (figure 1) employs a probing wave with a frequency of 280 GHz, together with a five-channel heterodyne receiver capable of providing full information on the frequency spectrum of measured signals [15]. A unique feature of the scattering geometry is the oblique propagation of the probing beam with respect to the magnetic field, with both probe and scattered waves lying nearly on the equatorial midplane (figure 2), so that the wave vectors of measured fluctuations are nearly perpendicular to the magnetic surfaces. However, they have also small components in both diamagnetic and toroidal directions, from which one can infer
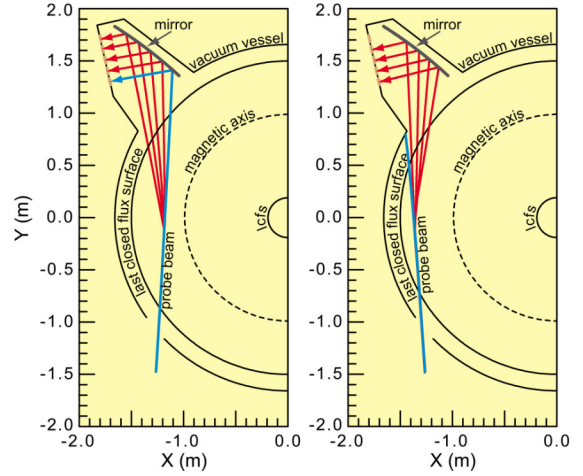
Figure 2. Probe beam (blue) and scattered waves (red) for detection of inboard (left) and outboard (right) fluctuations. Steerable optics can position the scattering region from the magnetic axis to the plasma edge.

the phase velocity of fluctuations in the poloidal plane.

This novel scattering geometry takes advantage of the large curvature of magnetic field lines and the strong anisotropy of turbulence in tokamaks, where short scale fluctuations are characterized by $k_\parallel \ll k_\perp$, with $k_\parallel$ and $k_\perp$ the wave vector components parallel and perpendicular to the magnetic field. This makes the instrumental selectivity function, i.e., the col-
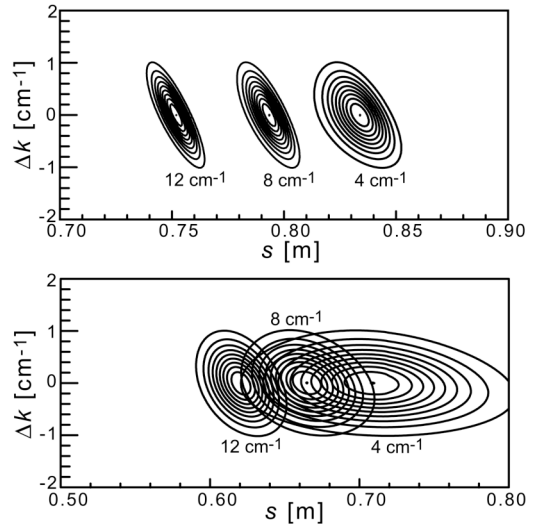

Figure 3. Contour plots (ten levels equally spaced from 0.1 to 1) of the instrumental selectivity as a function of the position along the probe beam (s) and the wave number mismatch (Δk) for the two configurations of figure 2 (top: inboard fluctuations, bottom: outboard fluctuations). Labels are wave numbers of measured fluctuations.

lection efficiency of scattered waves, strongly localized [16, 17], as illustrated in figure 3 showing the contour plot of the selectivity function along the trajectory of the probing beam for the two cases of figure 2. From this, we get that the radial footprint of the scattering region is smaller than the diameter of the probing beam (5.0 cm), so that the radial resolution of our measurements is ±2.5 cm. Figure 2 shows also a wave number resolution of ~ ±1 cm^{-1}

3. Results

The experimental results presented in this paper were obtained in plasmas with high harmonic fast wave (HHFW) heating [18,19]. Use of this radio frequency (RF) technique – where an electromagnetic wave with the frequency (30 MHz) of an ion cyclotron harmonic (~10th) is launched into NSTX where it is absorbed by the electrons – was motivated by its ability to produce electron temperature (T_e) profiles with large central values and steep gradients. An example is in figure 4, showing the electron temperature and density profiles in a Helium plasma with 1.2 MW of RF heating power, a minor radius of 0.65 m, a major radius of 0.85 m, an elongation of 2, a magnetic field of 0.55 T and a current of 700 kA. The latter values of magnetic field and plasma current were chosen for minimizing the spurious effects of MHD turbulence. Because of the low plasma density,
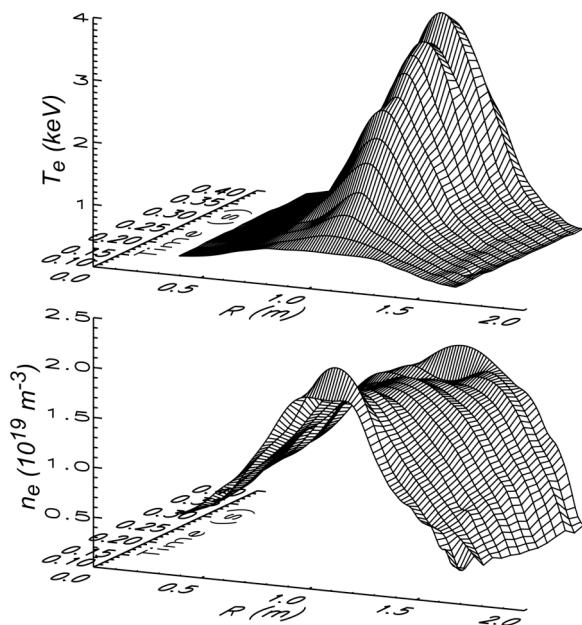
Figure 4. Electron temperature (top) and density (bottom) profiles with 1.2 MW of HHFW heating.
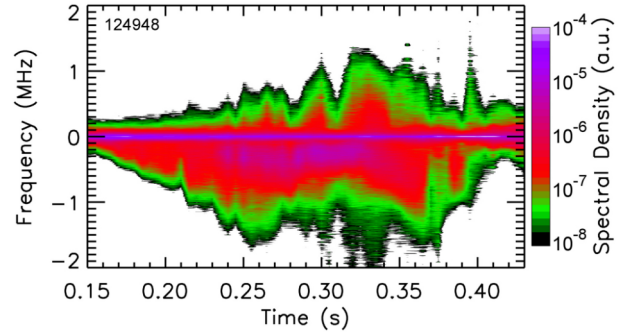
Figure 5. Logarithmic contour plot of the spectral density of fluctuations with $k_\perp \rho_e$=0.2-0.4 at R=1.2 m. Negative frequencies correspond to wave propagation in the electron diamagnetic direction.

i.e, a weak electron-ion coupling, the ion temperature (T_i) remained nearly constant (with central values of 0.8-1.0 keV).

Figure 5 shows the time evolution of the spectral density of measured fluctuations with $k_\perp$= 14 cm^{-1} at R =1.2 m, corresponding to the range of $k_\perp \rho_e$=0.2-0.4 (with ρ_e the electron gyroradius), $k_\perp \rho_s$=8.5-17 (with ρ_s the ion gyroradius at the electron temperature) and $k_\perp \rho_i$=8-10 (with ρ_i the ion gyroradius). The latter implies that the source of observed fluctuations is not the Ion Temperature Gradient (ITG) mode, which is instead characterized by $k_\perp \rho_i < 1$ [1-3]. This mode is also excluded by the frequency asymmetry of measured spectra, as shown in figure 5, indicating that fluctuations propagate in the electron diamagnetic direction.

It is interesting to note that for the plasma density in figure 4, $k_\perp \delta_{sk} \sim 2$, where δ_{sk} is the collisionless skin depth ($c/\omega_{pe} = \rho_e / \beta_e^{1/2}$, with ω_{pe} the plasma frequency and β_e the electron beta). This is not surprising since for sufficiently large values of β_e, such as those in the present experiment (3-6%), the characteristic turbulence scale length is expected to be of the order of the electron skin depth [4, 20].

The observed fluctuations appear to be related to the electron temperature gradient, as illustrated in figure 6 where the frequency integrated value of the spectral density (S_{tot}) of fluctuations in figure 5 is compared with the scale of T_e (defined as L_{T_e}=(dlnT_e/dr)$^{-1}$) at the radius of measurements. Note that plasma fluctuations begin to rise at the beginning of the RF pulse, when the value of L_{T_e} begins to

drop, and decrease towards the end of the pulse, when the opposite occurs.
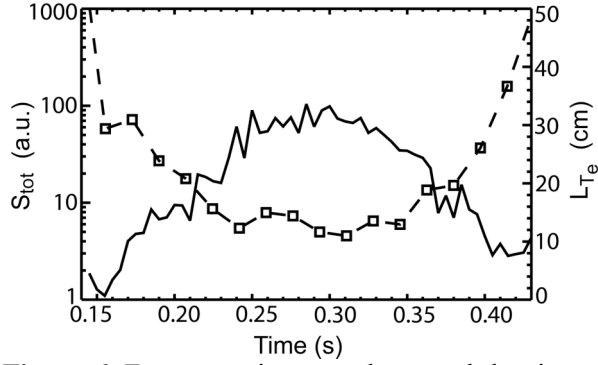
Figure 6. Frequency integrated spectral density S_{tot} (solid line) and radial scale L_{T_e} (dash line) for the case of figure 5.

The same phenomenon is illustrated in figure 7, showing the electron temperature profile and the spectrum of fluctuations at 0.3 s – when fluctuations are near their maximum value – and at 0.43 s – 30 ms after the end of the RF pulse when the electron temperature profile has collapsed and flattened on a wide central region. While both spectra contain a central narrow symmetric feature, which is caused by a spurious stray radiation, that at 0.3 s displays a strong Doppler shifted component, which is the signal of coherent wave scattering by plasma fluctuations. A difference of a factor of three in the value of L_{T_e} at the two times of measurement clearly demonstrates the dependence of plasma turbulence on the radial scale of T_e.
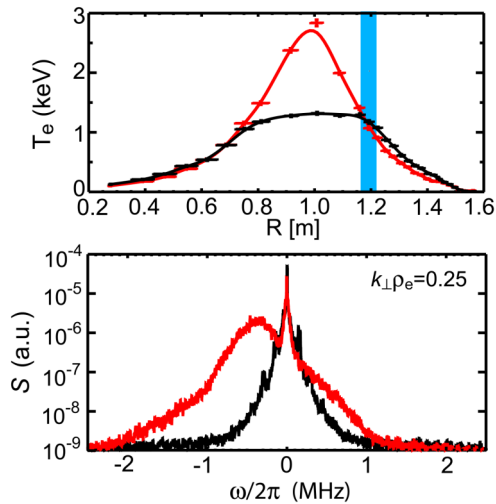

Figure 7. Temperature profiles (top) and spectral density of fluctuations (bottom) at 0.3 (red) and 0.43 s (black). Blue stripe (top) indicates the location of measurements where L_{T_e} is 15 and 50 cm, respectively. Negative frequencies (bottom) correspond to wave propagation in the electron diamagnetic direction.
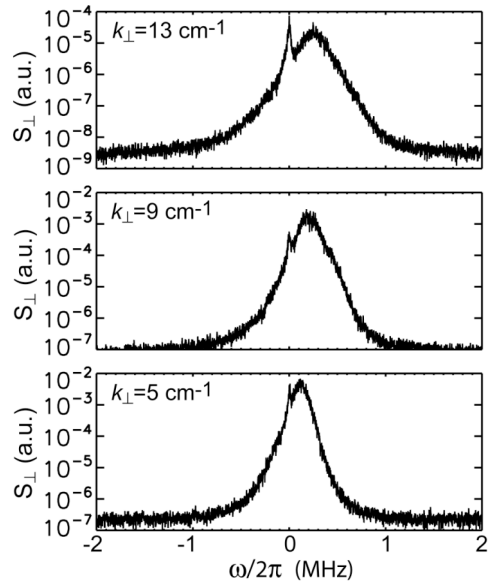

Figure 8. Spectral density of fluctuations in the range of wave numbers $k_\perp\rho_e$=0.1-0.2 at R=1.35 m. Positive frequencies correspond to wave propagation in the electron diamagnetic direction.

Short scale turbulent fluctuations were also detected on the outer region of the plasma column (R=1.35 m), as illustrated in figure 8 showing the spectral density of fluctuations with wave numbers in the range $k_\perp\rho_e$ =0.1-0.2 and $k_\perp\rho_i \approx k_\perp\rho_s$ = 4-8. Again, the scale length is of the order of the collisionless skin depth ($k_\perp\delta_{sk}$=1-2). As in the case of core fluctuations, wave numbers are outside the range of the ITG mode, and their propagation is in the electron diamagnetic direction (corresponding to positive frequencies for the scattering configuration used in these measurements).
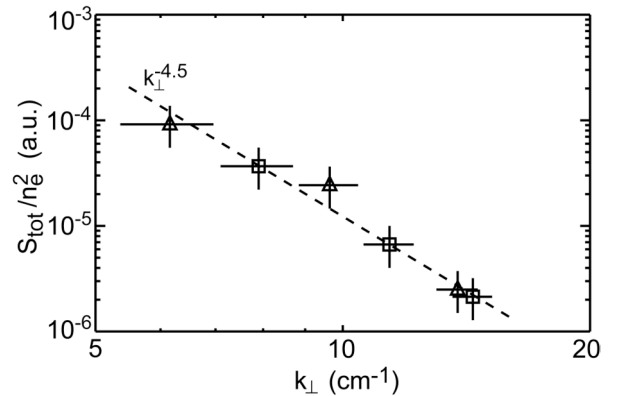
Figure 9. k-spectrum of density fluctuations (normalized to the square density) as a function of $k_\perp$ for both inboard (squares) and outboard (triangles) measurements.
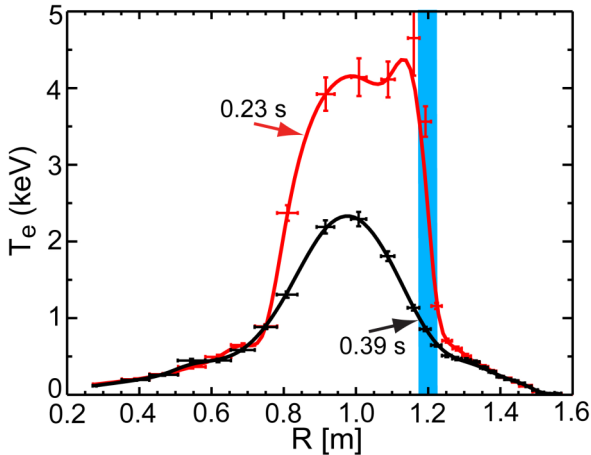
The power spectrum of measured fluctuations at t=0.3 s (i.e., the value of S_{tot} normalized to the square of the plasma density) is
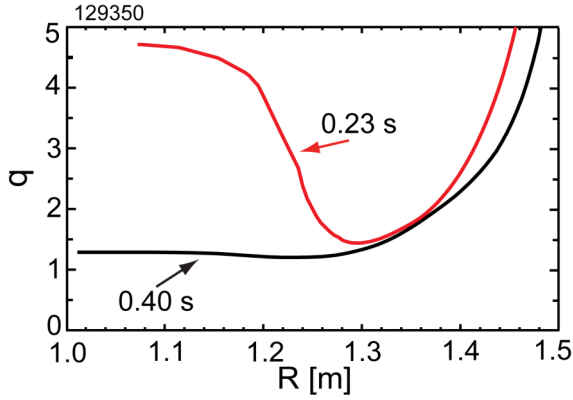
Figure 10. Magnetic safety factor (from MSE measurements) at the beginning (red) and the end (black) of RF pulse (3 MW).

shown in figure 9 as a function of $k_\perp$ for both inboard (figure 5) and outboard (figure 8) measurements. Surprisingly, the power spectrum seems to follow a similar power law ($\sim k_\perp^{-4.5}$) at both plasma locations in spite of different values of T_e (1.5 vs. 0.5 keV). If the measured turbulence is isotropic perpendicularly to the magnetic field – which our measurements cannot prove – the mean square density fluctuation would follow the power law $\left\langle \left| \tilde{n}_e^2 \right| \right\rangle / n_e^2 \propto k_\perp^{-3.5}$.

These results demonstrate the importance of the gradient of T_e for the existence of an electron gyro-scale turbulence in NSTX. However, another determining factor is the magnetic shear $s = r(d\ln q/dr)$ (where q is the magnetic safety factor) – especially if negative [6]. An example of the latter is shown in figure 10, resulting from 3 MW of HHFW heating during the early phase of a Deuterium plasma (0.2 s), when the toroidal current was still diffusing into the plasma core. A strong electron heating

together with a low ionic effective charge (1.4 vs. 2.5 in figure 4) had the effect of slowing down the current diffusion and producing a central region with strong negative shear (figure 10) that lasted for ~0.1 s, until the onset of an MHD instability caused a fast redistribution of the plasma current and a flattening of its density profile. During the phase of negative shear, the electron temperature developed a large gradient near the radius of minimum q (figure 11), where the value of L_{T_e} was much smaller than the lowest values in figure 6. This must be considered evidence of the existence of an internal transport barrier [21]. Figure 12 shows that fluctuations were suppressed at the transport barrier - a striking similarity to what was found in similar TFTR plasmas [22], albeit for fluctuations driven by the ion temperature gradient (ITG). However, turbulent fluctuations reappeared at the end of the heating pulse (figure 12) when the plasma current fully extended to the plasma core, making the q-profile nearly constant over a wide central region (figure 10).

Finally, neither plasmas with a strong negative shear nor with an internal transport barrier were observed when the RF power was injected at a later time (0.3 s).
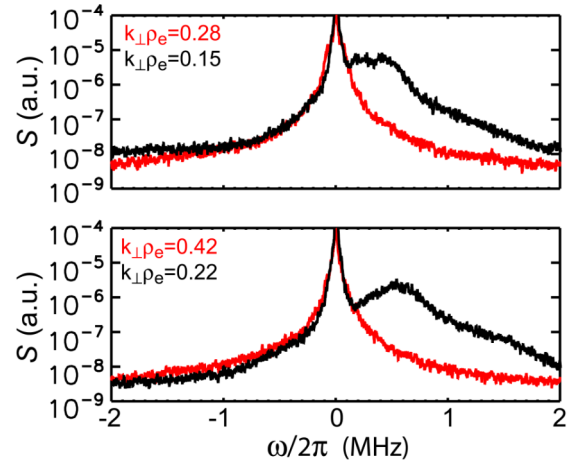
Figure 12. Same as in figure 10 for the measured fluctuations.

4. Discussion

In an attempt to determine the source of observed fluctuations, we employed a linear version of the GS2 stability code [23] to obtain the normalized critical gradient $(R/L_{T_e})_{crit}$ for the onset of the ETG instability. This code solves the gyrokinetic Vlasov-Maxwell equa-


Figure 11. Same as in figure 10 for the electron temperature.
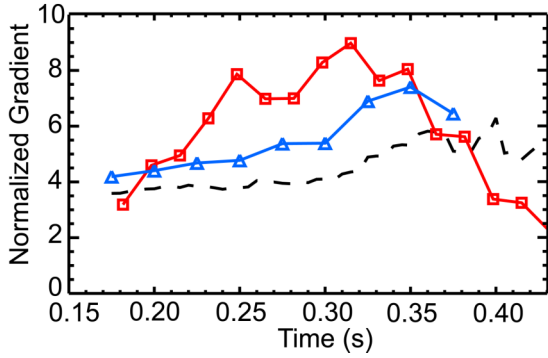
Figure 13. Time evolution of the measured gradient R/L_{T_e} (red) and GS2 critical gradient $(R/L_{T_e})_{crit}$ for the onset of the ETG mode (blue). Dash line is the critical gradient from [24].

tions, including passing and trapped particles, electromagnetic effects, as well as a Lorentz collision operator. The results are shown in figure 13, where the critical gradient is compared with the measured normalized temperature gradient R/L_{T_e} for the case of figure 5. From this, we conclude that the ETG mode is indeed unstable over most of the RF pulse where the critical gradient is smaller than the electron temperature gradient. Comparison with figure 6 shows that the level of measured fluctuations correlates with the departure of the temperature gradient from the critical gradient.

Figure 13 displays also an algebraic expression of the normalized critical gradient that was derived in [24] using a best fit of GS2 results for a set of model tokamak configurations [24]. This is given by

$$(R/L_{T_e})_{crit}=(1+Z_{eff}T_e/T_i)(1.3+1.9s/q)(1-1.5\varepsilon),$$

where Z_{eff} is the ionic effective charge and $\varepsilon=r/R$ is the inverse aspect ratio. This formula, showing the stabilizing role of the temperature ratio T_e/T_i and the magnetic shear,
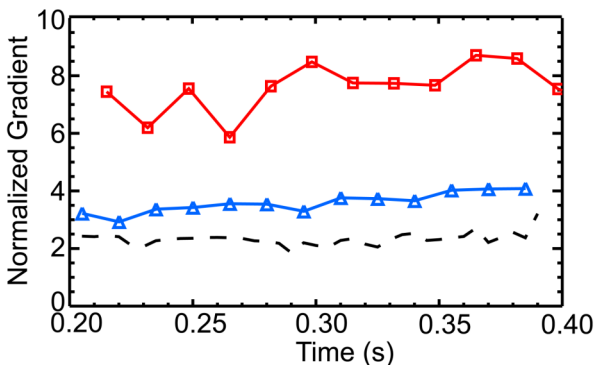
Figure 14. Same as in figure 13 for the case of figure 8.

gives values of critical gradient that are not very different from those obtained using the NSTX plasma configuration of our experiment.

Similar plots are displayed in figure 14 for the case of outboard fluctuations (figure 8), showing again that fluctuations coincide with a temperature gradient that is larger than the critical gradient. At this plasma location, however, since the HHFW heating did not modify significantly the plasma conditions, both the amplitude of measured fluctuations and the ETG critical gradient remained nearly constant in time.

Finally, we found that the GS2 code predicts stability for the ETG mode in the plasma region with strong negative shear of figure 10, in agreement with our fluctuation measurements (figure 12).

5. Conclusion

In conclusion, an electron gyro-scale turbulence was observed in NSTX plasmas in the range of wave numbers $k_\perp\rho_e$= 0.1-0.4, corresponding to a turbulence radial scale of the order of the collisionless skin depth. Large values of $k_\perp\rho_i$ and a strong correlation with the scale of T_e seem to exclude the ITG mode as the source of turbulence. Experimental observations and an agreement with numerical results from the linear gyrokinetic GS2 code support the conjecture that the observed turbulence is driven by the electron temperature gradient.

In plasmas with strong negative magnetic shear, the formation of an internal transport barrier was observed near the radius of minimum q, where no electron gyro-scale fluctuations were detected. This could be used as evidence of the role played by the turbulence described in this paper on plasma transport. However, additional experiments together with nonlinear numerical simulations of plasma turbulence (in progress) are needed before reaching any definite conclusion.

References

[1] B. Coppi and G. Rewoldt, in *Advances in Plasma Physics,* edited by A. Simon and W. B. Thompson (John Wiley and Sons, New York, 1976), Vol. 6, p. 421.

[2] W. Horton, Rev. Mod. Phys. **71**, 735 (1999).

[3] J. W. Connor and H. R. Wilson, Plasma Phys Control. Fusion **36,** 719 (1994).

[4] W. Horton, P. Zhu, G. T. Hoang, T. Aniel and X. Garbet, Phys. Plasmas **7**, 1494 (2000).

[5] W. Dorland, F. Jenko, M. Kotschereuther and B. N. Rotgers, Phys. Rev. Lett. **85**, 5579 (2000).

[6] F. Jenko and W. Dorland, Phys. Rev. Lett. **89**, 225001 (2002).

[7] W. M. Nevins, J. Candy, S. Cowley, T. Dannert, A. Dimits, W. Dorland, C. Estrada-Mila, G. W. Hammett, F. Jenko, M. J. Pueschel and D. E. Shumaker, Phys. Plasmas **13**, 122306 (2006).

[8] A. M. Dimits, W. N. Nevins, D. E. Shumaker, G. W. Hammett, T. Dannert, F. Jenko, M. J. Pueschel, W. Dorland, S. C. Cowley, J. N. Leboeuf, T. L. Rhodes, J. Candy and C. Estrada-Mila, Nucl. Fusion **47**, 817 (2007).

[9] R. E. Waltz, J. Candy, and M. Fahey, Phys. Plasma **14**, 0561116 (2007).

[10] W. Horton, G. T. Hoang, C. Bourdelle, X. Garbet, M. Ottaviani and L. Colas, Phys. Plasmas **11**, 2600 (2004).

[11] A. D. Gurchenko, E. Z. Gusakov, A. B. Altukhov, A. Yu. Stepanov, L. A. Esipov, M. Yu. Kantor, D. V. Kouprienko, V. V. Dyachenko and S. I. Lashkul, Nucl. Fusion **47**, 245 (2007).

[12] S. M. Kaye, R.E. Bell, D. Gates, B. P. LeBlanc, F. M. Levinton, J.E. Menard, D. Mueller, G. Rewoldt, S.A. Sabbagh, W. Wang and H. Yuh, Phys. Rev. Lett. **98**, 175002 (2007).

[13] E. Mazzucato, D. R. Smith, R. E. Bell, S. M. Kaye, J. C. Hosea, B. P. LeBlanc, J. R. Wilson, P. M. Ryan, C. W. Domier, N. C. Luhmann, Jr., H. Yuh, W. Lee and H. Park, Phys. Rev. Lett. **101**, 075001 (2008).

[14] M. N. Rosenbluth and N. Rostoker, Phys. Fluids **5**, 776 (1962).

[15] D.R. Smith, E. Mazzucato, W. Lee, H. Park, W. Domier and N. C. Luhmann, Jr., to be published in Rev. Sci. Instrum.

[16] E. Mazzucato, Phys. Plasmas **10**, 753 (2003).

[17] E. Mazzucato, Plasma Phys Control. Fusion **48,** 1749 (2006).

[18] J. Hosea, R. E. Bell, B. P. LeBlanc, C. K. Phillips, G. Taylor, E. Valeo, J. R. Wilson, E. F. Jaeger, P. M. Ryan, J. Wilgen, H. Yuh, F. Levinton, S. Sabbagh, K. Tritz, J. Parker, P. T. Bonoli and R. Harvey, Phys. Plasmas **15**, 056104 (2008).

[19] C. K. Phillips *et al.*, Paper EX/P6-25 at this Conference

[20] B. Coppi, in *Collective Phenomena in Macroscopic Systems*, edited by G. Bertin (World Scientific, Singapore, 2007).

[21] H. Y. Yuh, F. M. Levinton, S. M. Kaye, D. R. Smith, E. Mazzucato, H. K. Park, R. E. Bell, B. P. LeBlanc, J. C. Hosea and K. Tritz, Paper EX/P3-1 at this Coference

[22] E. Mazzucato, S. H. Batha, M. Beer, M. Bell, R. E. Bell, R. V. Budny, C. Bush, T. S. Hahm, G. W. Hammett, F. M. Levinton, R. Nazikian, H. Park, G. Rewoldt, G. L. Schmidt, E. J. Synakowski, W. M. Tang, G. Taylor and M. C. Zarnstorff, Phys. Rev. Lett., **77**, 3145 (1996).

[23] M. Kotschenreuther, G. Rewoldt, and W. M. Tang, Comput. Phys. Commun. **88**, 128 (1995).

[24] F. Jenko, W. Dorland and G. W. Hammett, Phys. Plasmas **8**, 4096 (2001).